2

X-911-74-60

PREPRINT

NASA TM X- 70649

ESTIMATION OF SEA SURFACE TEMPERATURE FROM REMOTE SENSING IN THE 11-13 μm WINDOW REGION

C. PRABHAKARA

G. DALU

V. G. KUNDE

FEBRUARY 1974

GSFC — GODDARD SPACE FLIGHT CENTER

GREENBELT, MARYLAND

(NASA-TM-X-70649) ESTIMATION OF SEA SURFACE TEMPERATURE FROM REMOTE SENSING IN THE 11-13 MICRON WINDOW REGION (NASA) 30 p HC $4.50 CSCL 08J

N74-25888

Unclas

G3/13 40598

30

ESTIMATION OF SEA SURFACE TEMPERATURE FROM REMOTE SENSING IN THE 11-13 μm WINDOW REGION

C. Prabhakara

G. Dalu

V. G. Kunde

February 1974

GODDARD SPACE FLIGHT CENTER

Greenbelt, Maryland

ESTIMATION OF SEA SURFACE TEMPERATURE FROM REMOTE SENSING IN THE 11-13 μm WINDOW REGION

C. Prabhakara, G. Dalu* and V. G. Kunde

ABSTRACT

The Nimbus 3 and 4 IRIS spectral data in the 11-13 μm water vapor window region are analysed to determine the sea surface temperature (SST). The high spectral resolution data of IRIS are averaged over approximately 1 μm wide intervals to simulate channels of a radiometer to measure the SST. In the present exploratory study three such channels in the 775-960 cm^{-1} (12.9 - 10.5 μm) region are utilized to measure SST over cloud-free oceans. However two of these channels are sufficient in routine SST determination. The differential absorption properties of water vapor in the two channels enable one to determine the water vapor absorption correction without detailed knowledge of the vertical profiles of temperature and water vapor.

The feasibility of determining the SST is demonstrated globally with Nimbus 3 data where cloud-free areas can be selected with the help of albedo data from the MRIR experiment on board the same satellite. The SST derived from this technique agrees with the measurements made by ships to about 1°C.

*NRC-Research Associate. Permanent address: C.N.R.-Istituto di Fisica dell'Atmosfera - Rome, Italy.

CONTENTS

ILLUSTRATIONS

ESTIMATION OF SEA SURFACE TEMPERATURE FROM REMOTE SENSING IN THE 11-13 μm WINDOW REGION

INTRODUCTION

One of the techniques used to measure the sea surface temperature (SST) from satellites involves observations of the brightness temperature in the 8-13μm water vapor window region under cloud-free sky conditions. Allison and Kennedy (1967), Smith et al.(1970), Shenk and Solomonson (1972), Rao et al. (1972) and others have estimated the SST from remote sensing window measurements. The principal advantage with this infrared window is that it can be used both night and day. A second advantage is that low noise equivalent temperature may be attained in radiometric measurements as the terrestrial emission has its peak value in this spectral region.

Several of the earlier attempts to estimate the SST from the window measurements have dealt elaborately with the problem of eliminating cloud contaminated data. The present study does not offer any improvement in this respect. The problem of correcting the window data for water vapor absorption however, is better resolved in this study.

The brightness temperature, measured from space over a cloud free ocean, in the window is in general lower than the SST. The water vapor absorption is mainly responsible for this effect. In the earlier studies the water vapor attenuation correction is derived from climatological data on water vapor and temperature in the atmosphere. Such climatological corrections can introduce errors as large as ±2°C in the estimated SST. It is necessary therefore to apply the water vapor correction corresponding to the local vertical distribution of temperature and water vapor to improve the accuracy of the estimated SST. Such soundings from a remote platform would require elaborate instrumentation and data reduction procedures.

Anding and Kauth (1970), and Price (1973) have examined the usefulness of differential absorption in the window region to correct for the water vapor absorption with soundings of temperature and water vapor. In this study a transmittance model for the water vapor window region is developed which can be used in a simple scheme that does not require temperature and humidity soundings of the atmosphere to estimate SST over cloud free oceans with the help of Nimbus 3 and 4 IRIS measurements. This scheme takes advantage of the differential absorption properties of the water vapor in the spectral region 775 - 960 cm^{-1}. With this technique the SST is estimated with an accuracy of about 1°C from IRIS measurements.

TRANSMISSION OF WATER VAPOR IN THE 11-13 μm REGION

It is necessary to model the water vapor absorption in the three spectral regions 775 - 831, 831 -887, and 887 - 960 cm^{-1} which are used to simulate the broad band radiometer channels for the retrieval of SST. The 1000 - 1100 cm^{-1} region has been avoided due to the strong ozone absorption. The effects of aerosols are not considered in this investigation.

The total water vapor transmission in the 11 μm window region may be expressed as

$$\tau(\nu, T) = \tau_e(\nu, T)\, \tau_p(\nu, T)\, \tau_\ell(\nu, T) \qquad (1)$$

where τ_e and τ_p are associated with the water vapor continuum and τ_ℓ with the water vapor lines.

The laboratory measurements of Bignell (1970) and Burch (1970) show that the water vapor absorption in the 8 - 13 μm window region is primarily dependent on the water vapor partial pressure e. This absorption is referred to as "e-type" absorption, one of its characteristics being a strong negative temperature dependence. Water dimer molecules may be responsible for this behavior. Window radiance measurements made by Platt (1972) with a radiometer on board an aircraft looking down at the sea surface and measurements made by Lee (1973) with a balloon borne radiometer, are consistent with the presence of the e-type absorption in the atmosphere. Nimbus 4 IRIS data reported by Kunde et al. (1974) also confirm this type of absorption. Grassl (1973) derived the magnitude of the aerosol and e-type absorption coefficients in the window region with the help of a ground based radiometer that measured the sky emission. The absorption coefficients deduced by Grassl are in close agreement with the laboratory data obtained by Bignell and Burch. Grassl also found that in temperate and cold climates, the aerosol absorption can be comparable to the e-type absorption. Wark (1972), Houghton and Lee (1972) and Prabhakara et al. (1972)

have emphasised the importance of "e" type absorption in determining the SST.

The e-type absorption coefficients in the three channels considered here are obtained from the measurements of Burch (1970) made at a temperature of 296°K. These absorption coefficients are assumed to decrease at a rate of 2% per 1°C (Bignell, 1970). That is

$$k_e(\nu, T) = k_e(\nu, 296)\,[1 - 0.02(T - 296)] \tag{2}$$

where k_e is the e-type absorption coefficient (g^{-1} cm^2),

ν is the wave number (cm^{-1}),

T is the temperature (°K).

The transmission τ_e is then calculated with the formula

$$\tau_e(\nu, T) = \mathrm{Exp}[-k_e(\nu, T)\, ew] \tag{3}$$

where e is the water vapor pressure (atm),

w is the path length of water vapor (g cm^{-2}).

The water vapor pressure in the atmosphere is assumed to decrease exponentially with height with a constant scale height. This assumption implies that the mean vapor pressure e in a column of the atmosphere is proportional to the total precipitable amount of water w in that column. That is

$$e = sw \tag{4}$$

where s is a constant.

As a working hypothesis it is assumed that a mean vapor pressure of 3 mb in an atmospheric column of 1 cm^2 corresponds to 1 gram of precipitable water in that column, which means $s = 3$ (mb g^{-1}).

With these numerical values and with the help of equations (2) and (3), we have calculated the transmission τ_e for different path lengths at two temperatures 280° K and 300° K.

The second component of the continuum absorption depends on the total pressure

$$\tau_p(\nu, T) = \mathrm{Exp}[-k_p(\nu, T)\, wp/p_0] \tag{5}$$

where

- k_p is the absorption coeefficient for the collision broadening in the wings of water vapor lines (g^{-1} cm^2),
- p is the average pressure of the layer of the atmosphere, weighted according to the distribution of water vapor, assumed to be 850 mb,
- p_0 is the standard pressure of 1000 mb.

Only upper limits have been inferred from the laboratory data for the value of k_p. In this study we have adopted the values of k_p used by Kunde and Maguire (1974). This component is only important for low water vapor concentrations ($w < 1$ g cm^{-2}).

For the spectral lines, Goody (1954) has listed the line data of Benedict and Kaplan (1959) arranged in 20 cm^{-1} intervals at three temperatures 220°, 260° and 300°K. These data are used to calculate the average transmission τ_ℓ due to spectral lines. A statistical band model with non-overlapping lines, having an exponential line intensity distribution, has been assumed,

$$\tau_\ell(\nu, T) = 1 - k_\ell w \left[1 + \frac{k_\ell w}{(4\alpha_0/\delta)\, p/p_0}\right]^{-1/2} \tag{6}$$

where $k_\ell = S/\delta$ is the mean absorption coefficient (g^{-1} cm^2),

S is the mean line intensity (g^{-1} cm),

δ is the average line spacing (cm^{-1}),

α_0 is the line half width at STP (cm^{-1}),

p is 850 mb,

p_0 is 1000 mb.

The absorption coefficients used are listed in Table 1 for two temperatures, 280° K and 300° K. The various transmission values derived in the three spectral intervals at the two different temperatures are shown in Table 2. The total transmission at the two temperatures is plotted in figs. 1a and 1b as a function of path length for the three spectral channels. From these figures it is seen that the transmission function to a first approximation is linearly related to the path length up to about 4 grams of precipitable water at both temperatures. This approximate linearity of the transmission is also obtained when we assume that the line intensity distribution has a form proposed by Godson (1954). As

Table 1

Water vapor absorption coefficients

Channel No.	$\Delta\nu$ (cm^{-1})	k_p (g^{-1} cm^2)		k_e (g^{-1} cm^2)		k_ℓ (g^{-1} cm^2)		α_0/δ
		280° K	300° K	280° K	300° K	280° K	300° K	STP
1	775-831	0.035	0.040	19.46	13.56	0.333	0.497	0.015
2	831-887	0.017	0.020	14.52	10.12	0.098	0.157	0.018
3	887-960	0.009	0.010	11.59	8.08	0.047	0.074	0.014

Table 2A

Water Vapor Transmissivities for 280° K

Channel		$\Delta\nu$	Precipitable water (g cm^{-2})						
			0.5	1	2	3	4	6	8
τ_p	1	775-831	0.985	0.970	0.942	0.914	0.887	0.835	0.787
	2	831-887	0.993	0.986	0.971	0.957	0.944	0.917	0.890
	3	887-960	0.996	0.992	0.985	0.977	0.970	0.955	0.940
τ_e	1	775-831	0.985	0.943	0.792	0.591	0.393	0.122	0.024
	2	831-887	0.989	0.957	0.840	0.676	0.498	0.208	0.062
	3	887-960	0.991	0.966	0.870	0.731	0.573	0.286	0.108
τ_ℓ	1	775-831	0.920	0.880	0.825	0.783	0.748	0.690	0.641
	2	831-887	0.963	0.939	0.905	0.878	0.856	0.820	0.790
	3	887-960	0.981	0.967	0.947	0.931	0.917	0.895	0.877
τ	1	775-831	0.893	0.805	0.615	0.423	0.261	0.070	0.012
	2	831-887	0.946	0.886	0.738	0.568	0.402	0.156	0.044
	3	887-960	0.968	0.927	0.812	0.665	0.510	0.244	0.089

Table 2B

Water Vapor Transmissivities for 300° K

Channel		$\Delta\nu$	Precipitable water (g cm^{-2})						
			0.5	1	2	3	4	6	8
τ_p	1	775-831	0.983	0.967	0.934	0.903	0.873	0.815	0.762
	2	831-887	0.992	0.983	0.967	0.950	0.934	0.903	0.873
	3	887-960	0.996	0.992	0.983	0.975	0.967	0.950	0.934
τ_e	1	775-831	0.990	0.960	0.850	0.693	0.521	0.231	0.074
	2	831-887	0.992	0.970	0.886	0.761	0.615	0.335	0.143
	3	887-960	0.994	0.976	0.908	0.804	0.678	0.418	0.212
τ_ℓ	1	775-831	0.899	0.851	0.784	0.733	0.691	0.620	0.560
	2	831-887	0.948	0.917	0.874	0.841	0.814	0.769	0.731
	3	887-960	0.972	0.954	0.928	0.909	0.892	0.865	0.842
τ	1	775-831	0.875	0.790	0.622	0.459	0.314	0.117	0.032
	2	831-887	0.933	0.874	0.749	0.608	0.468	0.233	0.091
	3	887-960	0.962	0.924	0.828	0.713	0.585	0.343	0.167

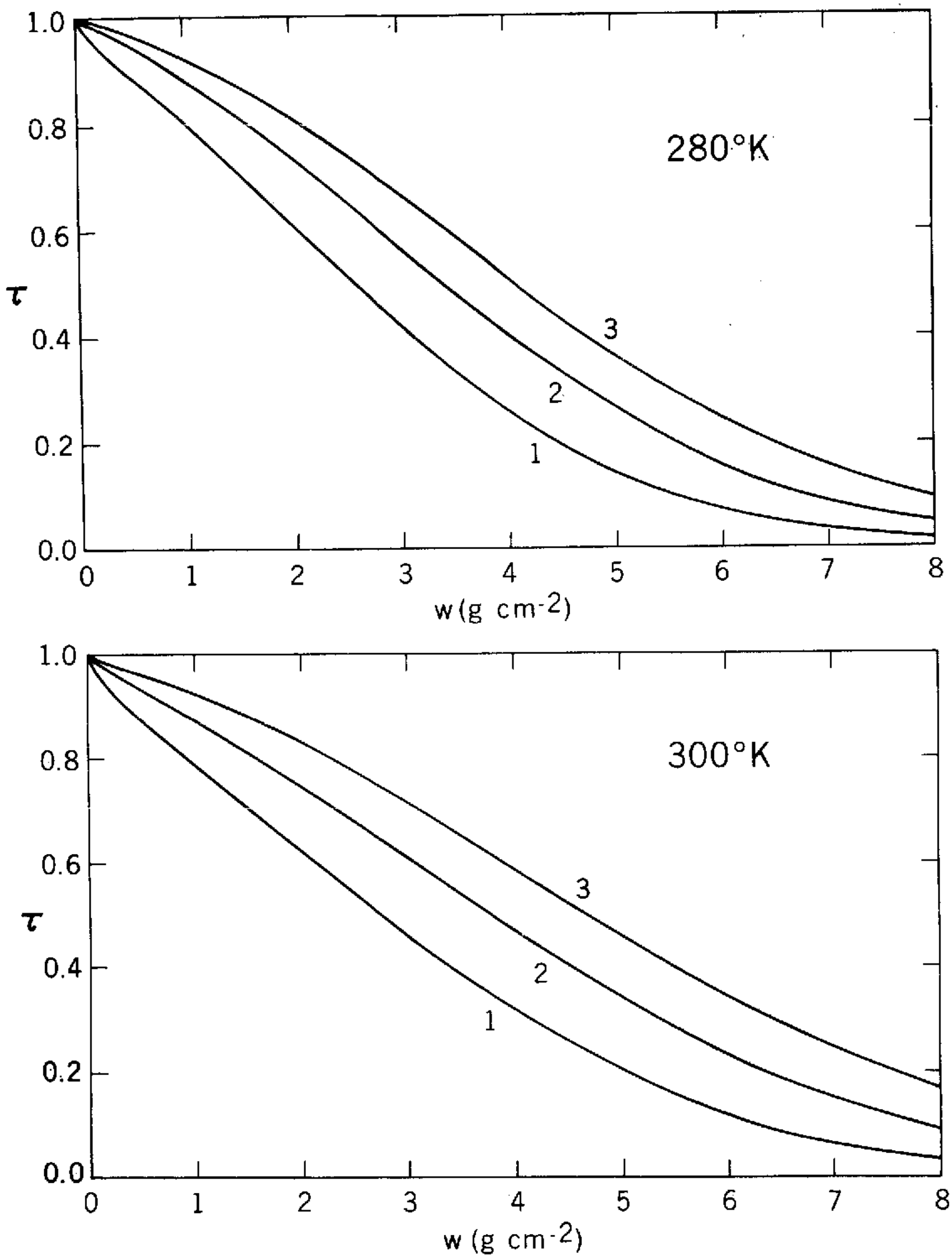

Figure 1. Water vapor transmission in the three channels; 1. 775–831 cm^{-1}, 2. 831–887 cm^{-1} and 3. 887–960 cm^{-1}; as a function of precipitable water content in the atmosphere for T = 280° K (a) and T = 300° K (b).

these temperatures and path lengths cover a wide variety of atmospheric conditions from tropics to high latitudes, it may be stated that this approximate linear law is applicable over most of the globe. Using the linear property of the transmission function shown in figs. 1a and 1b, the following equation is developed

$$\tau(\nu, w, T) \cong 1 - K(\nu)\, w(1 - \epsilon(T - 296)) \tag{7}$$

where $K(\nu)$ is an effective absorption coefficient corresponding to the total water vapor absorption and the coefficient ϵ accounts for the temperature dependence of $K(\nu)$.

The transmission functions derived here are dependent on the assumed water vapor distribution in the atmosphere, on the statistical band model, and on the absorption coefficients k_ℓ and k_p. For this reason the magnitude of $K(\nu)$ can change with the choice of the model and the parameters used in the calculations. However it is found that for a realistic combination of parameters, the transmission function $\tau(\nu)$ varies in a nearly linear fashion with respect to path length w. This property is exploited in the present study.

THEORY

In a cloud-free, non scattering atmosphere under local thermodynamic equilibrium, the radiative transfer equation for the upwelling intensity $I(\nu)$ may be written as

$$I(\nu) = B(\nu, T_s)\, \tau(\nu, p_0) + \int_{\tau(\nu, p_0)}^{1} B[\nu, T(p)]\, d\tau(\nu, p) \qquad (8)$$

where p_0 and p are surface pressure and pressure at any height (mb) respectively,

ν is the wave number (cm^{-1}),

T is the temperature (K),

T_s is the surface temperature (K),

B is the Planck intensity (erg cm^{-1} $ster^{-1}$ s^{-1}),

τ is the transmission from any pressure level p to the top of the atmosphere.

The surface emissivity in equation (8) is assumed to be unity.

The above equation may be simplified as

$$I(\nu) = B(\nu, T_s)\, \tau(\nu, p_0) + \bar{B}(\nu)\, [1 - \tau(\nu, p_0)] \qquad (9)$$

where $\bar{B}(\nu)$ is the weighted mean Planck emission of the atmosphere

$$\bar{B}(\nu) = \int_{\tau(\nu, p_0)}^{1} B[\nu, T(p)]\, d\tau \Bigg/ \int_{\tau(\nu, p_0)}^{1} d\tau \qquad (10)$$

Substituting equation (7) into equation (9), we get

$$I(\nu) \cong B(\nu, T_s) - AK(\nu)\, [B(\nu, T_s) - \bar{B}(\nu)] \qquad (11)$$

where $A = w\,[1 - \epsilon(T(p) - 296)]$ is a constant for a given atmosphere, independent of wave number.

The Planck function B can be expanded about the surface temperature T_s with only the linear terms retained to yield

$$B(\nu, T) \cong B(\nu, T_s) + \frac{\partial B(\nu, T_s)}{\partial T} (T - T_s) \tag{12}$$

This approximation holds good over a small range of temperatures and a narrow wave number span. With this approximation equation (11) becomes

$$T(\nu) \cong T_s - AK(\nu) [T_s - \overline{T}(\nu)] \tag{13}$$

where $T(\nu)$ is the brightness temperature and $\overline{T}(\nu)$ is the equivalent radiative temperature of the atmosphere.

Equation (13) indicates a linear relationship between the observed brightness temperature and the absorption coefficient $K(\nu)$, provided that $\overline{T}(\nu)$ is not strongly dependent on ν. With the help of the radiative transfer equation (8), model calculations based on typical atmospheric temperature and humidity profiles were made to examine the amount by which $\overline{T}(\nu)$ changes with ν. It is found from these model calculations, that within the 775–960 cm^{-1} region, $\overline{T}(\nu)$ changes with ν by less than 1°C. The magnitude of $(T_s - \overline{T}(\nu))$ is found to be about 10°C. In view of this, the change in $\overline{T}(\nu)$ is neglected in equation (13) to arrive at an approximate linear relationship between $T(\nu)$ and $K(\nu)$ as follows

$$T(\nu) \cong T_s - \beta K(\nu) \tag{14}$$

where $\beta = A [T_s - \overline{T}(\nu)]$ is a constant for a given atmosphere.

Now if we know the brightness temperature $T(\nu)$ in at least two spectral regions, which have appreciable difference in $K(\nu)$, equation (14) can be used to estimate the sea surface temperature T_s. This formulation does not require explicitly either the temperature and humidity distribution in the atmosphere, or the temperature and pressure dependence of the absorption coefficients.

RESULTS AND DISCUSSION

The Nimbus 4 IRIS had a $\sim$ 95 km field of view, 2.8 cm^{-1} spectral resolution and noise equivalent radiance of about 0.5 erg cm^{-1} $ster^{-1}$ s^{-1} (Hanel et al., 1972). These high spectral resolution data reveal the influence of numerous water vapor absorption lines, which are strong in the tropics and decrease in strength at high latitudes. In addition these spectra indicate that the brightness temperature increases steadily from about 775 cm^{-1} to 960 cm^{-1}. This is illustrated in Fig. 2 where a few spectra selected over cloud-free ocean are shown. The cloud-free condition is inferred from the Nimbus 4 Image Dissector Camera System (IDCS) pictures (Sabatini, 1970). This procedure is somewhat subjective and is not practical for collecting a large sample of cloud-free spectra. A small sample of 8 clear sky spectra was selected where sea surface temperature was available from ship measurements. The mean brightness temperature corresponding to each one of the spectral channels 775-831, 831-887 and 887-960 cm^{-1} is listed in Table 3. From this sample of IRIS data and the corresponding observed sea surface temperature, one can determine the relative values of the three absorption coefficients $K(\nu)$ from equation (14) for each of

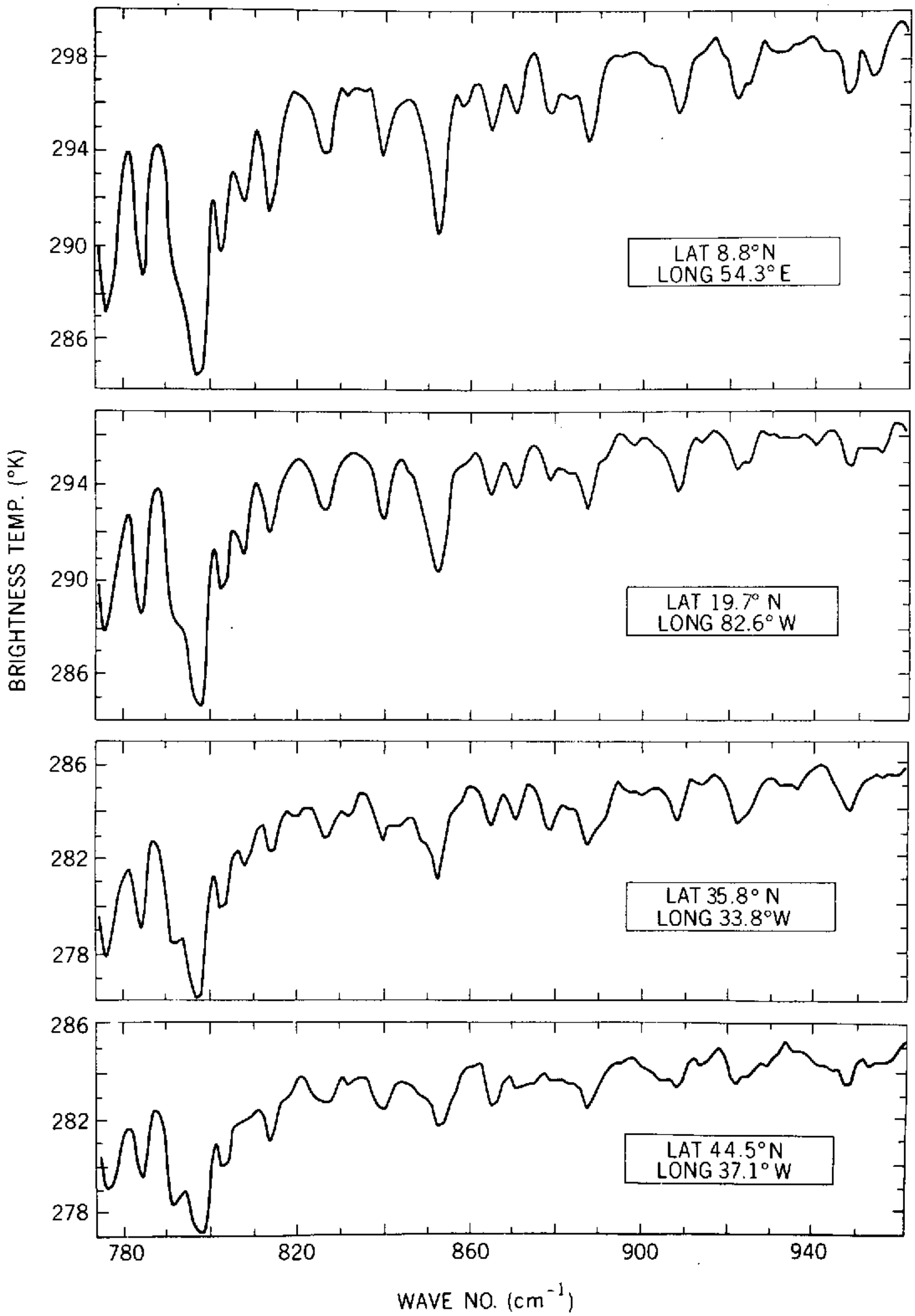

Figure 2. Cloud free Nimbus 4 IRIS brightness temperature spectra.

Table 3

Nimbus 4 IRIS window brightness temperature, and the SST from IRIS and ships.

No.	Lat.	Long.	T_1	T_2	T_3	T_{IRIS}	T_{SHIP}
1	41.0°N	62.5°W	272.9	275.2	276.8	281.2	281.0
2	36.6°N	60.9°W	284.5	286.9	287.9	292.0	290.5
3	11.0°N	53.5°W	287.8	291.7	293.4	300.1	300.5
4	35.6°N	33.8°W	281.2	283.8	285.0	289.6	291.0
5	44.6°N	37.1°W	280.9	283.1	284.0	287.7	287.0
6	19.7°N	82.6°W	291.2	294.2	295.6	300.7	301.5
7	15.1°N	144.7°W	292.7	294.9	296.1	300.1	301.2
8	39.4°N	69.1°W	286.9	290.6	291.8	298.0	296.2

Table 4

Relative absorption coefficient (g^{-1} cm^2) for the three window channels

Channel	1	2	3
$\Delta\nu$	775-831	831-887	887-960
$K(\nu)$	0.191	0.131	0.104

the three spectral intervals. A first guess for these coefficients is derived from the synthetic transmission function illustrated in Figure 1a and these values are then adjusted to give a best fit to the data of Table 3. These values of $K(\nu)$ are listed in Table 4. In Fig. 3 a plot of the measured brightness temperatures versus $K(\nu)$ for the 8 cases is presented to show the degree of linearity in the observed data.

The advantage of using the method presented here to determine the SST is that it is inherently capable of taking into account the effects of water vapor and temperature profiles satisfactorily. This capability is particularly necessary in measuring the SST with meaningful accuracy over the tropics where the water vapor absorption correction is large and quite variable in time and space. To demonstrate this point a set of 6 cloud free Nimbus IRIS spectra from one orbit, from 8°N to 14°N along 55°E longitude on May 10, 1970, over Arabian Sea, are analysed. The window brightness temperature in the three channels for each of these 6 spectra is plotted in Fig. 4, as a function of the absorption coefficient $K(\nu)$. The intercept on the ordinate gives the value of the SST. It may be noticed that the IRIS window brightness temperature in the most transparent channel (887-960 cm^{-1}) increases by about 3°K going northward from 8°N to 14°N. One would erroneously infer from water vapor correction based on climatological atmospheric temperature and humidity data an increase, in the SST, of about 3°K from 8°N to 14°N. However, with the present correction scheme the estimated SST does not increase towards the north; instead it shows a small

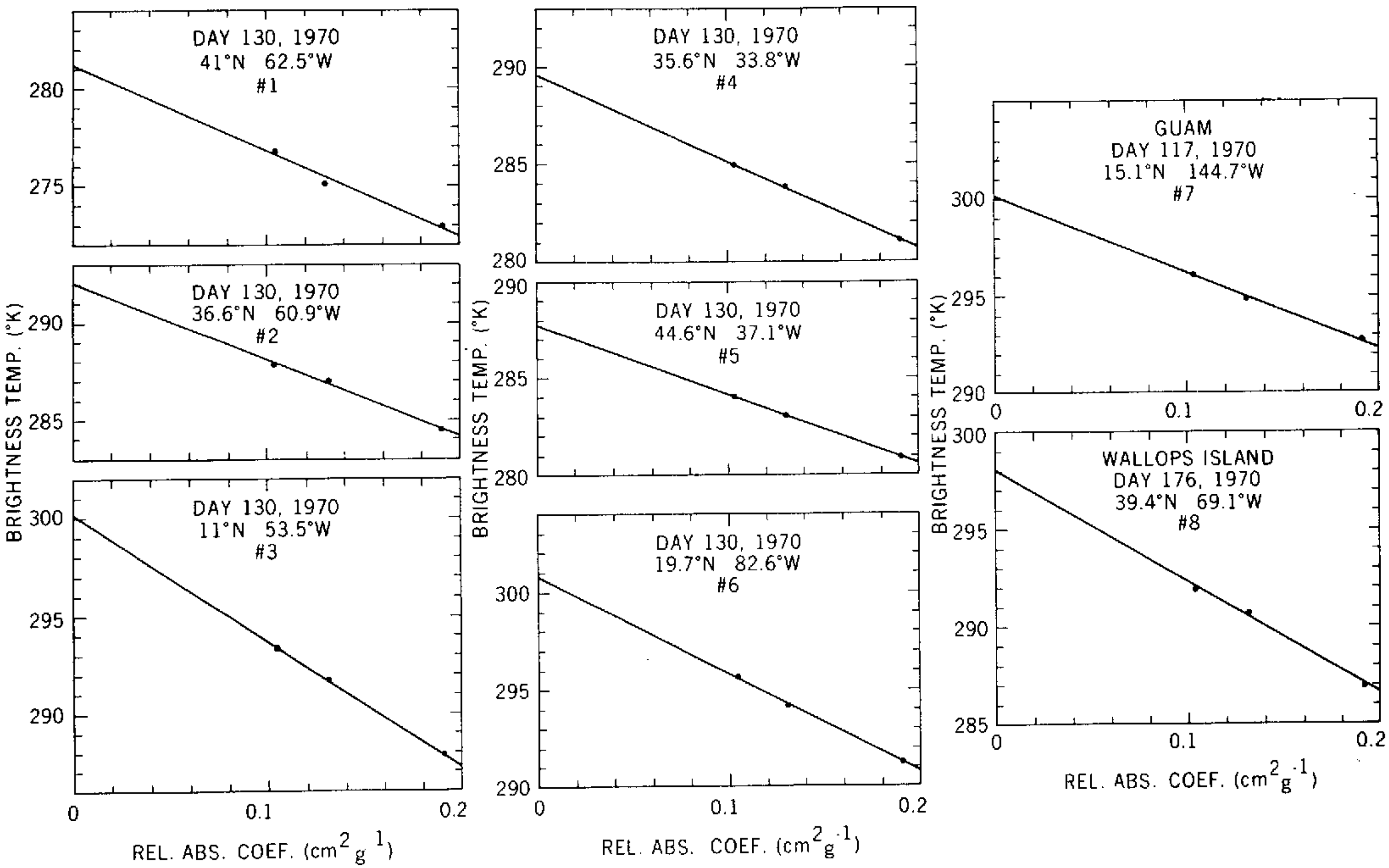

Figure 3. IRIS window brightness temperature versus relative absorption coefficient.

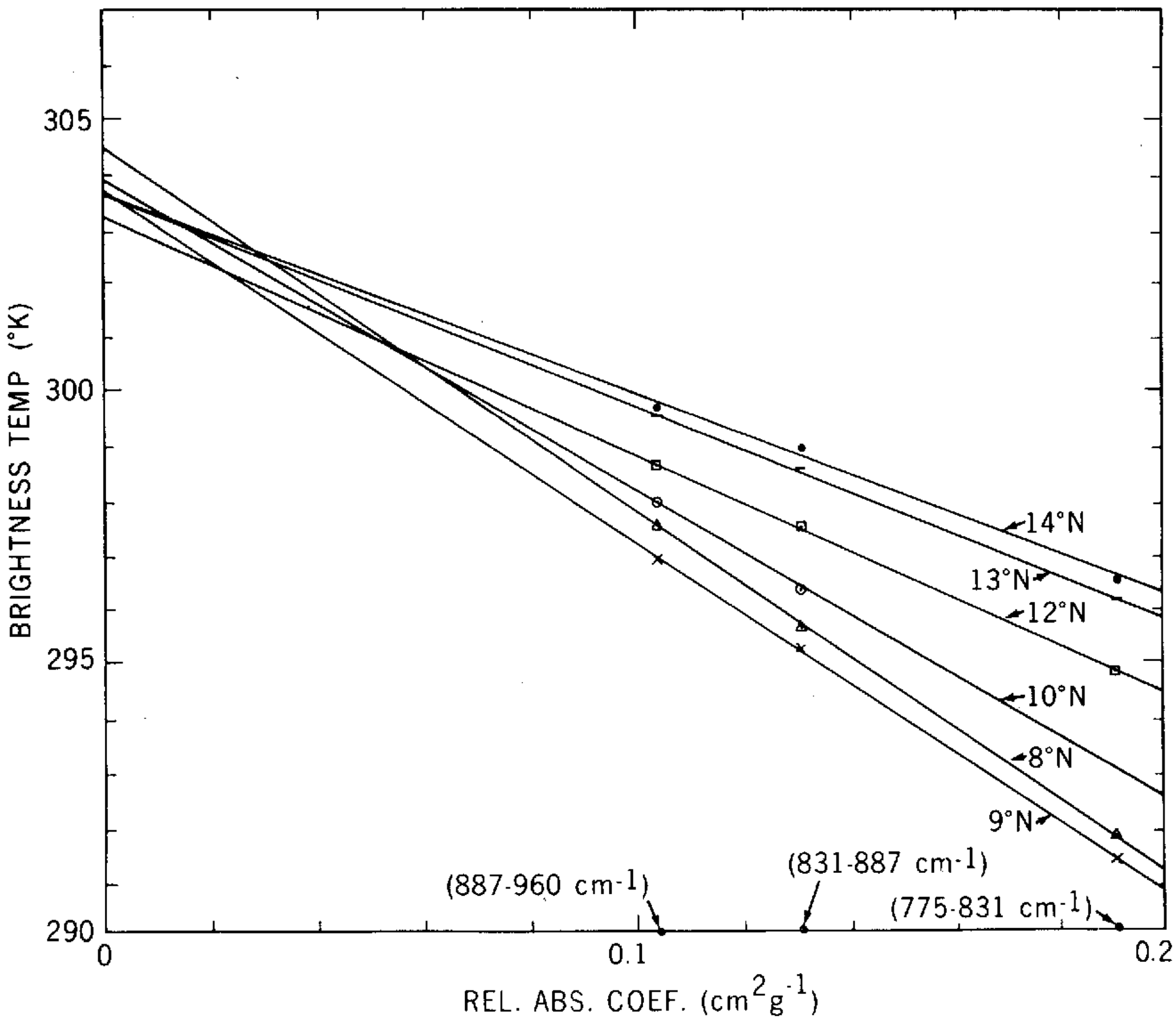

Figure 4. Window brightness temperature variation over the Arabian Sea between 8° N to 14° N along 55° E longitude on May 10, 1970, from Nimbus 4.

decrease of about 1° in agreement with the seasonal pattern (U.S. Naval Oceanographic Office, 1967) for that oceanic region.

The Nimbus 3 IRIS had a $\sim$150 km field of view, 5 cm^{-1} spectral resolution and noise equivalent radiance of about 1 erg cm^{-1} $ster^{-1}$ s^{-1} (Hanel and Conrath, 1969). These data, although slightly inferior to the Nimbus 4 IRIS measurements, can serve as good check on the validity of the method and the magnitude of the coefficients $K(\nu)$ because we can objectively select cloud free data in the following fashion. Measurements from the Nimbus 3 satellite, of a scanning Medium Resolution Infrared Radiometer (MRIR), with a field of view of about 50 km at nadir, included the reflected solar radiation in the visible and the infrared radiation in the 11 μm region (Sabatini, 1969). Clouds can reflect solar radiation in significant amounts while the ocean surface cannot. Thus with the help of the MRIR reflected solar radiation measurements at the nadir, it is possible to objectively select cloud-free IRIS data. During a period of 10 days in April 1969, a sample of 106 IRIS measurements over the oceans was extracted when corresponding ship measurements of the sea surface temperatures were available within ±1° of latitude and longitude. These data covered the globe from 60° S to 60° N. The SST derived from these IRIS data are compared with the ship data in Fig. 5. We see that over a wide dynamic temperature range of about 40° F to 85° F, the two sets of data agree very well. The R.M.S. difference between the two sets of data is about 2.5° F or 1.3° C. However the SST measured by ships has an error of about 1° C (Saur, 1963) and so the IRIS-SST measurements should have an accuracy better than 1.3°C.

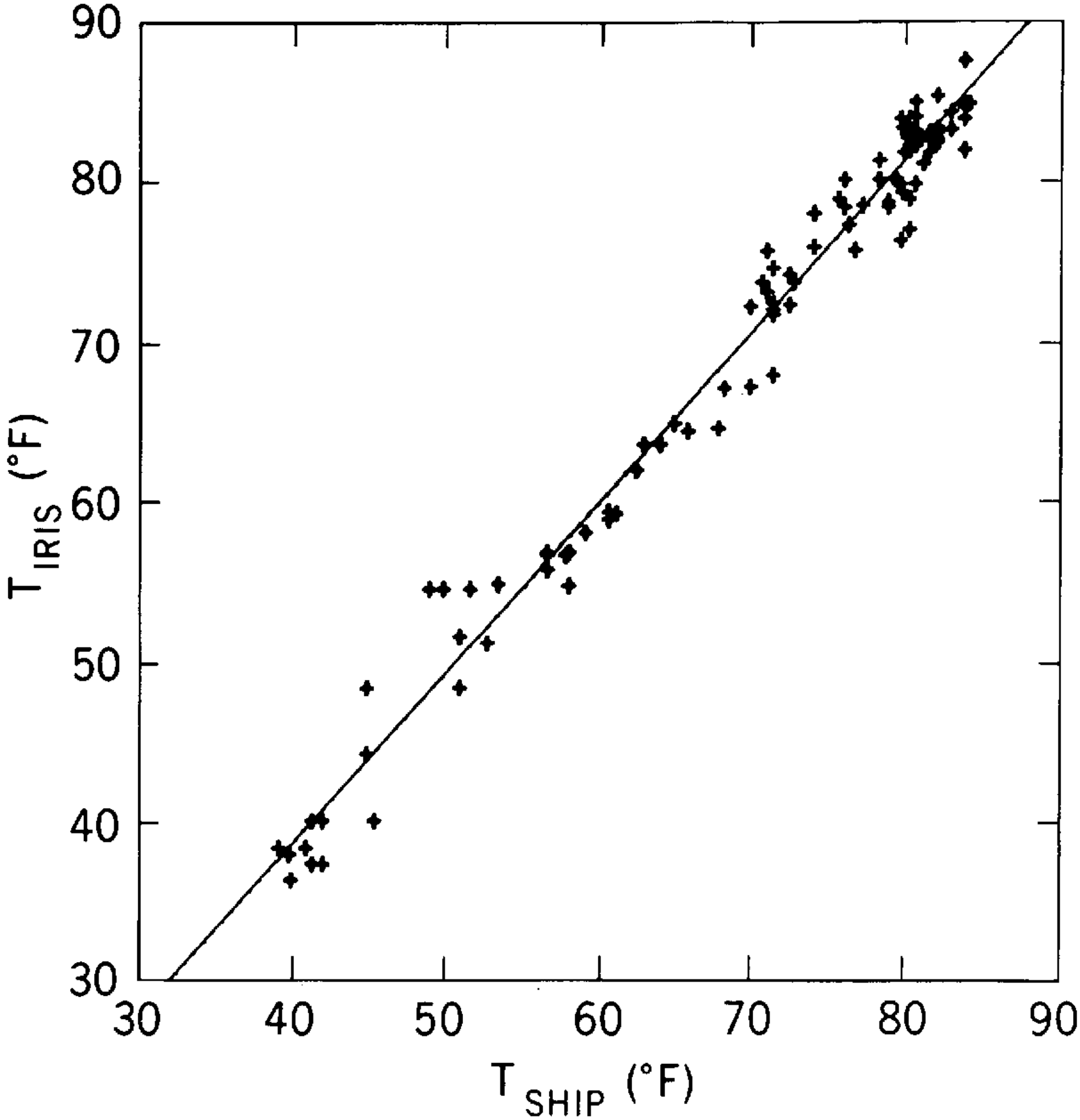

Figure 5. Comparison of SST derived from Nimbus 3 IRIS vs. ship measurements.

In order to examine if there is any systematic bias in the IRIS-SST with respect to ship measurements, a linear regression analysis is performed to obtain a line of best fit as shown in Fig. 5. One can notice that this regression line does not coincide with the line of perfect agreement which would be inclined at 45° to the axes. It appears that the use of $K(\nu)$ given in Table 4 leads to a slight underestimation of the SST over cold water of high latitudes and an over-estimation of the SST in the tropics. A further refinement in the magnitude of $K(\nu)$ eliminates this systematic bias and improves the accuracy of determining SST to about 1° C.

CONCLUSION

The basic result of this study is that over cloud free oceans we can make use of the differential water vapor absorption properties of the 11 μm window region to correct for the atmospheric attenuation. This correction scheme inherently takes into account the temperature and humidity structure prevailing at the location. Although three measurements in the window region 775-960 cm^{-1} were used to demonstrate this method, in principle two measurements are sufficient. The two window measurements may preferably be in the approximate regions 775-831 and 887-960 cm^{-1} to obtain the maximum effect of differential absorption.

The spatial and temporal changes of sea surface temperature in the tropics are generally small (about 2° C). The water vapor absorption correction over the tropics could range from about 4° to 8° C. Hence the technique of estimating the SST proposed in this study would be particularly valuable over the tropical oceans.

As the radiometric errors are amplified in the derived results, it would be desirable to have a radiometer capable of measuring brightness temperature accurate to 0.1° K in order to estimate the SST with an accuracy of about 0.5° K.

The scheme presented here can be adopted to any existing sea surface temperature measurement program, based on one window channel, by adding one more channel in the window.

ACKNOWLEDGMENT

The authors are thankful to Drs. A. Arking and B. J. Conrath, for many useful discussions, and to Lt. Col. R. A. Neff of USAF Environmental Technical Applications Center for the help in obtaining the ship measurements.

REFERENCES

Allison, L. J. and J. Kennedy, An evaluation of sea surface temperature as measured by the Nimbus I high resolution infrared radiometer, NASA Technical Note # D-4078, National Aeronautics and Space Administration, Washington, D.C., 25, 1967.

Anding, D. and R. Kauth, Estimation of Sea Surface Temperature from Space, Remote Sensing of the Environment, Vol. 1, No. 4, New York, N.Y., 217-220, 1970.

Benedict, W. S. and L. D. Kaplan, Calculation of line widths in H_2O-N_2 collisions, J. Chem. Phys., 30, #2, 388-399, 1959.

Bignell, K. J., The water vapour infra-red continuum, Quart. J. R. Met. Soc., 96, 390-403, 1970.

Burch, D. E., Semiannual technical report-Investigation of the absorption of infrared radiation by atmospheric gases, Philco-Ford Corporation, Aeronutronic Division, Publication No. U-4784, 27, 1970.

Godson, W. L., Spectral models and the properties of transmission functions, Proc. Toronto meteor. Conf., 1953, 35-42, 1954.

Goody, R. M., Atmospheric Radiation I. Theoretical Basis, Oxford, Clarendon Press, 1964.

Grassl, H., Separation of atmospheric absorbers in the 8-13 micrometer region, Beiträge zur Physik der Atmosphäre, 46, 75-88, 1973.

Hanel, R. A. and B. J. Conrath, Interferometer experiment on Nimbus 3: Preliminary results, Science, 165, 1258-1260, 1969.

Hanel, R. A., B. J. Conrath, V. G. Kunde, C. Prabhakara, I. Revah, V. V. Salomonson, and G. Wolford, The Nimbus 4 Infrared Spectroscopy Experiment, J. Geophys. Res., 77, 2629-2641, 1972.

Houghton, J. T. and A. C. Lee, Atmospheric Transmission in the 10-12 μm Window, Nature Physical Science, 238, 117-118, 1972.

Kunde, V. G., B. J. Conrath, R. A. Hanel, W. C. Maguire, C. Prabhakara and V. V. Salomonson, The Nimbus 4 Infrared Spectroscopy Experiment, 2. Comparison of Observed and Theoretical Radiances from 425-1450 cm^{-1}, J. Geophys. Res., 79, 777-784, 1974.

Kunde, V. G. and W. C. Maguire, Direct integration transmittance mode, Accepted for publication in J. Q. S. R. T., 1974.

Lee, A. C. L., A study of the continuum absorption within the 8-13 μm atmospheric window, Quart. J. R. Met., Soc., 99, 490-505, 1973.

Platt, C. M. R., Airborne Infrared Radiance Measurements (10 to 12 Micron Wavelength) of Tropical East-Coast Australia, J. Geophys. Res., 77, 1697-1609, 1972.

Prabhakara, C., B. S. Conrath and V. G. Kunde, Estimation of sea surface temperature from remote measurements in the 11-13 μm window region, NASA X-651-72-358, 1972.

Price, J. C., Analysis of some methods for obtaining sea surface temperature from satellite observations, NASA X-651-73-108, 1973.

Rao, P. K., W. L. Smith and R. Koffer, Global Sea-Surface Temperature Distribution Determined From an Environmental Satellite, Monthly Weather Review, 100, #1, 10-14, 1972.

Sabatini, R. R., The Nimbus 3 Users Guide, Nimbus Proj. Office, Goddard Space Flight Center, Greenbelt, Md., 1969.

Sabatini, R. R., The Nimbus 4 Users Guide, Nimbus Proj. Office, Goddard Space Flight Center, Greenbelt, Md., March 1970.

Saur, J. F. T., A study of the quality of sea water temperatures reported in logs of ships weather observations, J. Appl. Meteorol., 2, 417, 1963.

Shenk, W. E. and V. V. Solomonson, A multispectral technique to determine sea surface temperature using Nimbus 2 data, Jour. of Phys. Oceanography, 2, #2, 157-167, 1972.

Smith, W. L., P. K. Rao, R. Koffler and W. R. Curtis, The determination of sea surface temperature from satellite high resolution infrared window radiation measurements, Monthly Weather Review, 98, #8, 604-611, 1970.

U. S. Naval Oceanographic Office, 'Monthly Charts of Mean, Minimum, and Maximum Sea Surface Temperature of the Indian Ocean,' SP-99, Naval Oceanographic Office, Washington, D.C. 20309, 48 pages, 1967.

Wark, D. Q., Atmospheric transmittance used in indirect soundings of the earth's atmosphere, Proceedings of the International Radiation Symposium, Sendai, Japan, May 26-June 2, p. 554, 1972.